Journal of Applied Phycology (2020) 32:329–337
https://doi.org/10.1007/s10811-019-01941-3

Alkaline flocculation of *Microcystis aeruginosa* induced by calcium and magnesium precipitates

Tomáš Potočár[1] · João Augusto Vitorino Pereira[1] · Irena Brányiková[2] · Magdalena Barešová[3] · Martin Pivokonský[3] · Tomáš Brányik[4]

Received: 24 July 2019 / Revised and accepted: 26 September 2019 / Published online: 25 November 2019

Abstract

The biotechnological potential of *Microcystis aeruginosa* brings requirements for efficient cultivation and harvesting of biomass. Flocculation of *M. aeruginosa* at alkaline pH induced by calcium or magnesium precipitates was studied under model conditions, in culture medium with/without cellular organic matter (COM). The effect of independent variables (Ca^{2+}, Mg^{2+}, PO_4^{3-}, and pH) on the zeta potential and turbidity of cells and inorganic precipitates was quantified by response surface methodology. The experimentally obtained flocculation efficiencies (FEs) were compared with predictions of physicochemical interaction (DLVO) models. The results presented here delimited the concentration ranges of Ca^{2+}, Mg^{2+}, PO_4^{3-}, and pH, resulting in FE > 85%. The DLVO prediction model suggested that for high FE, positively charged precipitates and sufficient precipitate turbidity were required. At pH 10, alkaline flocculation was more advantageous using magnesium precipitates, since it required less phosphate. High FE with COM was achieved at pH 12 when precipitate formation was induced at a low phosphate concentration by the addition of magnesium hydroxide.

Keywords Cyanobacteria · Inorganic precipitates · Surface interactions · DLVO theory

Introduction

The presence of algae and cyanobacteria is considered necessary and common in aquatic environments (Wang et al. 2013); however, eutrophication and climate change have led to the increasing occurrence of algal blooms in natural waters (Ito et al. 2018). This phenomenon is expanding to become a worldwide threat to ecological integrity (Paerl et al. 2011). One of the most common cyanobacteria responsible for bloom formation is *Microcystis aeruginosa*, producing a wide range of cyanotoxins. These include hepatotoxins, neurotoxins and dermatotoxins (Merel et al. 2013). For these reasons, there has been a concerted effort to develop methods for removing *M. aeruginosa* from natural waters. These include flocculation (Shi et al. 2016; Lürling et al. 2017), magnetic separation (Lin et al. 2015), and flotation (Yap et al. 2014).

However, new challenges concerning biomass harvesting have emerged in connection with the increasing biotechnological potential of *M. aeruginosa* and its cyanotoxins. This encompasses the application of biomass as a feedstock for bioethanol production (Khan et al. 2016, 2017), a source of microcystin as an enzyme regulator (Tappan and Chamberlin 2008), a potential anticancer treatment (Niedermeyer et al. 2014), and a source of cyanotoxins as analytical standards (Lawton and Edwards 2008). Targeted cultivation of *M. aeruginosa* and the production of microcystins in photobioreactors (Geada et al. 2017a) requires the application of effective harvesting methods.

Due to the small size and low harvesting concentrations of *M. aeruginosa* (Geada et al. 2017b), centrifugation is expensive (Molina Grima et al. 2003). Preconcentration of cell suspensions by flocculation methods can improve the economics of harvesting cyanobacteria (González-Fernández and Ballesteros 2013). Alkaline flocculation induced by an increase in pH, related to both CO_2 depletion (Sukenik and Shelef 1984; Nguyen et al. 2014) and the addition of calcium/magnesium hydroxide (Folkman and Wachs 1973; Leentvar and Rebhun 1982) is not suited for removal of

✉ Tomáš Brányik
tomas.branyik@vscht.cz

[1] Department of Biotechnology, University of Chemistry and Technology Prague, Prague, Czech Republic

[2] Institute of Chemical Process Fundamentals, The Czech Academy of Sciences, Prague, Czech Republic

[3] Institute of Hydrodynamics, The Czech Academy of Sciences, Prague, Czech Republic

[4] Department of Biotechnology, University of Chemistry and Technology Prague, Technicka 5, 166 28 Prague, Czech Republic

harmful *Microcystis* sp. from surface waters, but it has been reported as possible preconcentration method for microalgae in biotechnological applications. The latter is using cheap slaked lime instead of more expensive chemical flocculants (Vandamme et al. 2012). The mechanism of alkaline flocculation was shown to be based on either neutralization of the surface charge on cells by oppositely charged colloidal precipitates or a favorable balance of apolar and polar interaction energies (Branyikova et al. 2018).

The colloidal scale of interacting particles allows to evaluate the flocculation of cyanobacteria by alkaline pH induced inorganic salt precipitates using the colloidal DLVO (Derjaguin-Landau-Verwey-Overbeek) model (Prochazkova et al. 2013), which quantifies interaction energies between surfaces by Lifshitz-van der Waals (LW) and electrostatic (EL) forces as a function of separation distance (Hermansson1999). Agreement between the DLVO model and flocculation tests can help in understanding the mechanism of flocculation.

Literature is lacking on the application of colloidal physicochemical interaction models to study forced alkaline flocculation of cyanobacteria. This paper presents experimental and modelling data on the importance of zeta potential, size of interacting particles, quantity of precipitates formed, pH, ionic strength, and components of medium, as well as cellular organic matter on interactions between cells and precipitates.

Material and methods

Microorganism, cultivation, and preparation of cell suspension

A sample of a freshwater cyanobacterium *M. aeruginosa* SAG 17.85 was obtained from the Culture Collection of Algae (http://sagdb.uni-goettingen.de).

The strain was grown in sterile Z8 medium (http://ccala.butbn.cas.cz/en/z-medium) in batch mode and at room temperature. The cultivations were carried out in 1-L flasks and aerated at 0.3 vvm with 0.2 μm filtered air. The culture was subjected to 12-h light/dark cycles with a photon flux of 55 μmol photons m^{-2} s^{-1} (QSL-2101, Biospherical Instruments Inc., USA) at room temperature. After 30 days of cultivation at a biomass concentration of 0.65 ± 0.08 g L^{-1}, cyanobacterial suspensions were centrifuged (4427×*g*, 15 min, 22 °C) and washed twice with distilled water. The separated cells were used for surface characterization and flocculation tests.

Experimental design and response surface methodology

The quantification of the impact of independent variables (Ca^{2+} or Mg^{2+}, PO_4^{3-}, and pH) on zeta potential (ZP) and turbidity (T) of precipitates was carried out using response surface methodology (RSM). The effects of ionic strength (IS) and pH on the ZP of *M. aeruginosa* were determined too. The variables were changed over three levels (Table 1) resulting in an experimental (alpha face centred small central composite) design (Table 2). The experimental data were treated with multiple regression analyses (Design Expert software, Stat-Ease Inc., USA) and statistically analyzed using ANOVA. Multiple regression analysis of flocculation efficiencies, as affected by ZP and T of precipitates, was carried out with Statistica software (Dell Inc, USA).

Zeta potential measurement

Precipitate samples were obtained by adding $CaCl_2$ or $MgCl_2$ and KH_2PO_4 into 250 mL of deionized water and adjusting the pH to 8–12 with 1 mol L^{-1} KOH. ZP values obtained after 5 min of stirring (magnetic stirrer, 1.5 cm in length, 200 rpm, 25 °C) had the final value ± 5% and were evaluated by RSM.

The cell suspensions were prepared in KCl with ionic strengths (10–40 mmol L^{-1}) and pH corresponding to conditions used for characterization of precipitates.

Zeta potentials of *M. aeruginosa*, Ca^{2+} and Mg^{2+} precipitates were measured at least in triplicate using the Zetasizer Nano-ZS (Malvern, UK) at 25 °C. The Helmholtz-Smoluchowski equation (Kolska et al. 2012) was used to calculate the results, and the maximum experimental error was ± 2.8 mV.

Turbidity and cell size measurement

Precipitate samples were prepared and agitated for 5 min as in zeta potential measurement. Turbidity was measured by a laboratory hazemeter (MZN-93-MC2, Charles University, Czech Republic) at 25 °C. Measurements were carried out in triplicate at an angle of 15°, and the results were expressed in formazine turbidity units (FTUs). The maximum experimental error was ± 6%. The cell size of *M. aeruginosa* was determined by image analysis (Prochazkova et al. 2013). Solubility

Table 1 Independent variables, their coded levels, and actual values

Symbol	Independent variables (units)	Coded level		
		− 1	0	+ 1
Ca	Ca^{2+} (mmol L^{-1})[a]	0.5	3.0	5.5
Mg	Mg^{2+} (mmol L^{-1})[b]	0.5	3.0	5.5
P	PO_4^{3-} (mmol L^{-1})[a,b]	0.05	0.20	0.35
pH	pH[a,b,c]	8	10	12
IS	Ionic strength (mmol L^{-1})[c]	10	25	40

[a] Variables for characterisation of Ca^{2+} precipitates

[b] Variables for characterisation of Mg^{2+} precipitates

[c] Variables for characterisation of *M. aeruginosa* cells

Table 2 Central composite design matrix and response values of average zeta potentials (ZP) of *M. aeruginosa* cells and precipitate particles, and turbidities (T) of Ca^{2+} and Mg^{2+} precipitate particles as a result of variations in Ca^{2+} (Ca) or Mg^{2+} (Mg) and PO_4^{3-} (P) concentrations, ionic strength (IS), and pH

Run	Variables				Responses		
	Ca[a]/ Mg[b]	P[a,b]	IS[c]	pH[a,b,c]	ZP[a/b] [mV]	T[a/b] [FTU]	ZP[c] [mV]
1	− 1	− 1	− 1	− 1	− 4.4/− 7.9	0.12/0.60	− 47.6
2	+ 1	− 1	+ 1	− 1	10.3/− 5.2	0.48/0.56	− 31.5
3	0	0	0	− 1	5.3/− 5.2	0.60/0.52	− 45.1
4	− 1	+ 1	–	− 1	− 1.5/− 9.9	0.72/0.60	–
5	+ 1	+ 1	–	− 1	9.7/− 4.3	1.68/0.60	–
6	0	− 1	+ 1	0	10.1/7.0	1.32/0.68	− 32.1
7	− 1	0	− 1	0	− 6.5/− 14.4	3.88/0.64	− 47.7
8	0	0	0	0	10.4/2.6	2.64/0.92	− 45.0
9	+ 1	0	–	0	11.1/4.9	3.00/1.28	–
10	0	+ 1	–	0	9.2/1.8	5.80/1.60	–
11	− 1	− 1	+ 1	+ 1	− 9.1/− 1.0	1.56/4.56	− 33.2
12	+ 1	− 1	− 1	+ 1	9.3/2.1	1.12/47.36	− 52.1
13	0	0	0	+ 1	4.3/− 2.0	1.76/17.16	− 50.7
14	− 1	+ 1	–	+ 1	− 26.8/− 25.3	7.76/3.48	–
15	+ 1	+ 1	–	+ 1	6.5/− 1.5	4.08/34.36	–

[a] Variables for characterization of Ca^{2+} precipitates

[b] Variables for characterization of Mg^{2+} precipitates

[c] Variables for characterization of *M. aeruginosa* cells

equilibria of inorganic species in model solutions were calculated with Visual MINTEQ, version 3.1. (KHT, Sweeden) and presented as equilibrium amount of solids precipitated at the given conditions.

Flocculation experiments

Harvesting of cyanobacteria by alkaline pH induced flocculation was tested on cell suspensions (0.5 ± 0.02 g L^{-1}) (Table 3), in which the pH was adjusted (pH 8–12) with 1 mol L^{-1} KOH. Flocculation tests were performed in 18 × 180 mm glass test tubes with 25 mL of *M. aeruginosa* cell suspensions. The suspension was vortexed for 10 s at 2500 min^{-1} (IKA Vortex 3, Germany) and left still for 30 min. Subsequently, sample was taken level at the centre of the test tubes (2 cm below the liquid) and the absorbance A_1 (750 nm) was measured (Infinite 200 PRO, Tecan, Switzerland). The flocculation efficiency (FE, %) was calculated as $FE = [(A_0 - A_1)/A_0] \times 100$, where A_0 is the initial absorbance at 750 nm (Geada et al. 2017b) of the cyanobacterial suspension.

The standard flocculation tests (SFTs) were carried out in solutions, which contained $CaCl_2$ or $MgCl_2$ and KH_2PO_4 (Table 1). Experiments investigating the effect of cellular organic matter (COM) were performed under conditions defined in Table 3. The applied COM concentration of 50 mg L^{-1} (expressed as dissolved organic carbon (DOC)) was always added into SFT solutions prior to pH adjustment. Furthermore, SFTs were also carried out with the addition of fresh Z8 medium components.

All experiments were performed in triplicate with a maximum experimental error of ± 4%. Standard flocculation tests with Ca precipitates (runs 5, 8, 9, and 13, Table 3) had a maximum experimental error of ± 8%.

Statistical analysis of flocculation tests (two-way analysis of variance), with significance statements based on a probability of $p < 0.05$, was carried out with MS Excel software.

Isolation and characterization of cellular organic matter

M. aeruginosa cells were separated from the culture medium by filtration through 0.22-mm membrane filters (Millipore, USA). The separated cells were rinsed with deionized water (200 mL) and disrupted with ultrasonication followed by filtration (Pivokonsky et al. 2014). The extract was then concentrated tenfold in a rotary evaporator (Laborota 4000, Germany) at 20 °C and 16 mBar. The concentrated cellular organic matter (COM) obtained was stored at − 60 °C.

The isolated COM was characterized through the content of peptide/protein and non-peptide fractions (Safarikova et al. 2013) and dissolved organic carbon (DOC) content (Naceradska et al. 2017).

Table 3 Flocculation efficiency (FE) of *M. aeruginosa* cells as a result of variations in Ca^{2+} (Ca), Mg^{2+} (Mg), and PO_4^{3-} (P) concentrations, and pH during different flocculation tests

Run	Variables			FE[a] [%]	FE[b] [%]	FE[c,d] [%]	FE[e,f] [%]
	Ca[a]/ Mg[b]	P	pH				
1	− 1	− 1	− 1	3.7	4.8	–	–
2	+ 1	− 1	− 1	2.5	6.0	–	–
3	0	0	− 1	2.3	6.6	–	–
4	− 1	+ 1	− 1	2.3	3.1	–	–
5	+ 1	+ 1	− 1	64.1	4.8	–	–
6	0	− 1	0	20.7	10.8	–	–
7	− 1	0	0	24.7	1.6	–	–
8	0	0	0	78.8	20.9	–	–
9	+ 1	0	0	74.0	86.5	97.5[d]	59.4[f]
10	0	+ 1	0	89.8	92.5	96.9[c]	72.7[e]
11	− 1	− 1	+ 1	5.35	94.5	–	–
12	+ 1	− 1	+ 1	52.6	99.9	–	93.1[f]
13	0	0	+ 1	80.4	97.9	–	–
14	− 1	+ 1	+ 1	7.1	6.8	–	–
15	+ 1	+ 1	+ 1	95.5	99.9	–	88.8[e]

[a] Standard flocculation test (SFT) with Ca^{2+} precipitates
[b] SFT with Mg^{2+} precipitates
[c] SFT with Ca^{2+} precipitates and addition of medium components
[d] SFT with Mg^{2+} precipitates and addition of medium components
[e] SFT with Ca^{2+} precipitates and addition of COM (50 mg L^{-1} DOC)
[f] SFT with Mg^{2+} precipitates and addition of COM (50 mg L^{-1} DOC)

Results

Zeta potential of cells and precipitate particles

A determination of surface charges of cyanobacteria and Ca^{2+}/Mg^{2+} precipitates was carried out to facilitate the interpretation of flocculation tests and obtain input data for subsequent model predictions.

The surface charge (ZP) of *M. aeruginosa* cells was negative over a range of ionic strengths (IS) and pH values with more negative ZP values at low IS (Table 2). The ANOVA analysis for ZP of *M. aeruginosa* showed that the model was highly significant ($F = 68.3$, $p = 0.0027$) (Table 4). The analysis also revealed the significance ($p < 0.05$) of both linear factors (IS, pH) and the quadratic term IS^2 in predicting the ZP response (Table 4). Statistically insignificant ($p > 0.1$) was the interactive term IS×pH and quadratic term pH^2. The final equation for ZP of *M. aeruginosa*, expressed in terms of actual factors, is:

$$ZP = -71.57 + 7.3854 \times \mathrm{pH} - 1.05935 \times IS + 0.02375 \times pH \times IS - 0.4479 \times pH^2 + 0.0277 \times IS^2$$

Table 4 ANOVA for response surface quadratic model of zeta potential of *M. aeruginosa* cells in a model solution (KCl) of different ionic strengths and pH

	SSQ	*df*	MSQ	*F* value	*p* value (Pro>*F*)
Model	537.6	5	107.5	68.3	0.0027
IS	428.4	1	428.4	272.3	0.0005
pH	23.0	1	23.0	14.6	0.0315
IS×pH	2.0	1	2.0	1.3	0.3385
IS^2	77.7	1	77.7	49.4	0.0059
pH^2	6.4	1	6.4	4.1	0.1367
Res.	4.7	3	1.6		
CT	542.3	8			
R^2	0.9913				
Adj.R^2	0.9768				

SSQ sum of squares, *df* degrees of freedom, *MSQ* mean square, *Res.* residual, *CT* correction total

The ZP of precipitates, formed by pH shift from pH 7 to pH 8-12 in solutions containing Ca^{2+} and PO_4^{3-}, was in the range from − 26.8 to 11.1 mV, while for Mg^{2+} and PO_4^{3-}, it was from − 25.3 to 7.0 mV (Table 2). As predicted by Visual MINTEQ, the only precipitate formed from Ca^{2+} and PO_4^{3-} at pH 8–12 should be hydroxyapatite (HA, equilibrium amount of solid HA from 1.66×10^{-5} to 1.16×10^{-4} mol L^{-1}). The effect of Ca^{2+} and PO_4^{3-} concentrations and pH on ZP of HA and the ANOVA analysis of the experimental data was presented in Branyikova et al. (2018).

The ZP of Mg^{2+} precipitates was negative at high PO_4^{3-} and low Mg^{2+} values and vice versa. This was more pronounced at pH 10 and 12. The ANOVA analysis of data revealed that the model for ZP of Mg^{2+} precipitates was highly significant ($F = 7.06$, $p = 0.0222$) (Table 5). Multiple regression analysis showed the significance ($p < 0.05$) of two linear factors (Mg^{2+} (Mg), PO_4^{3-} (P)) and the interactive pH×P term. Statistically less significant terms ($0.05 < p < 0.1$) were pH×Mg, Mg^2, and pH^2 (Table 5). The final equation predicting the ZP of Mg^{2+} precipitates, expressed in terms of actual factors, is:

$$ZP = -134.9736 + 25.844 \times pH + 1.2989 \times Mg + 24.5415 \times P + 0.542 \times pH \times Mg - 12.4365 \times pH \times P + 6.8925 \times Mg \times P - 1.2295 \times pH^2 - 0.967 \times Mg^2 + 135.8996 \times P^2$$

Turbidity of precipitate particles

A determination of the turbidity (T) of Ca^{2+}/Mg^{2+} precipitates induced by alkaline pH was carried out to quantify the number of precipitate particles. Multiple regression of T values (Table 2) led to a model for T of Ca^{2+} precipitates presented in Branyikova et al. (2018).

Table 5 ANOVA for response surface quadratic model of zeta potential of precipitates in a model solution with different concentrations of Mg^{2+} (Mg) and PO_4^{3-} (P) and pH

	SSQ	*df*	MSQ	*F* value	*p* value (Pro>*F*)
Model	920.9	9	102.3	7.06	0.0222
pH	6.18	1	6.18	0.43	0.5425
Mg	329.4	1	329.4	22.74	0.0050
P	138.2	1	138.2	9.54	0.0272
pH×Mg	58.8	1	58.8	4.06	0.1000
pH×P	111.3	1	111.3	7.69	0.0392
Mg×P	53.45	1	53.45	3.69	0.1128
pH^2	62.2	1	62.2	4.29	0.0930
Mg^2	93.96	1	93.96	6.49	0.0515
P^2	24.04	1	24.04	1.66	0.2540
Res.	72.43	5	14.5		
CT	993.3	14			
R^2	0.9271				
Adj.R^2	0.7958				

SSQ sum of squares, *df* degrees of freedom, *MSQ* mean square, *Res.* residual, *CT* correction total

Table 6 ANOVA for response surface quadratic model of turbidity of precipitates in a model solution with different concentrations of Mg^{2+} (Mg) and PO_4^{3-} (P) and pH

	SSQ	*df*	MSQ	*F* value	*p* value (Pro>*F*)
Model	2920.4	9	324.5	12.18	0.0066
pH	1307.8	1	1307.8	49.10	0.0009
Mg	530.6	1	530.6	19.92	0.0066
P	3.5	1	3.5	0.13	0.7316
pH×Mg	655.2	1	655.2	24.60	0.0043
pH×P	6.06	1	6.06	0.23	0.6536
Mg×P	3.28	1	3.3	0.12	0.7401
pH^2	294.1	1	294.2	11.04	0.0209
Mg^2	0.4	1	0.4	0.014	0.9117
P^2	1.2	1	1.2	0.044	0.8420
Res.	133.2	5	26.6		
CT	3053.6	14			
R^2	0.9564				
Adj.R^2	0.8779				

SSQ sum of squares, *df* degrees of freedom, *MSQ* mean square, *Res.* residual, *CT* correction total

At pH 8, the solubility equilibria calculations did not predict Mg^{2+} precipitate formation, although low turbidity values (0.52–0.60) were experimentally obtained. At pH 10 under conditions of run 9 (Table 2), the model solution was predicted to result in the formation of solid brucite (0.64 mmol L^{-1}) and $Mg_3(PO_4)_2$ (0.16 mmol L^{-1}). Under the most alkaline conditions (pH 12) of run 15, the only solid precipitate was brucite (5.49 mmol L^{-1}).

The model for T of Mg^{2+} precipitates was very significant (Table 6, $p = 0.0066$). As confirmed by multiple regression analysis, the turbidity caused by Mg^{2+} precipitate formation was influenced the most significantly ($p < 0.05$) by pH and Mg^{2+} (Mg) values, their interaction term pH×Mg and quadratic term pH^2. The other terms of the quadratic equation were statistically insignificant ($p > 0.1$) (Table 6). The final equation for T of Mg^{2+} precipitates, expressed in terms of actual factors, is:

$$T = 251.7348 - 52.6098 \times pH - 15.2056 \times Mg + 18.1635 \times P + 1.81 \times pH \times Mg - 2.9 \times pH \times P - 1.7067 \times Mg \times P + 2.6739 \times pH^2 + 0.06 \times Mg^2 + 30.025 \times P^2$$

Flocculation experiments

Flocculation experiments (standard flocculation tests) were carried out under alkaline conditions (pH 8–12) in the presence of either Ca^{2+} and PO_4^{3-}, or Mg^{2+} and PO_4^{3-} ions. These tests were planned in order to define favourable ratios between Ca^{2+}/Mg^{2+} and PO_4^{3-} at different pHs and compare the experimental data with DLVO model predictions.

During flocculation with Ca^{2+} precipitates at pH 8, the FE varied from 2.3 to 64.1% (Table 3). The highest FE (run 5, 64.1%) was achieved for positively charged Ca^{2+} precipitates (9.7 mV, T = 1.68, Table 2) due to the interaction between oppositely charged surfaces and a sufficient amount of Ca^{2+} precipitate. This can be demonstrated by comparing runs 2 and 5, where the Ca^{2+} precipitates had comparably positive ZP (cells had negative ZP), but in run 2, the T value was only 28.6% of that in run 5.

Even higher FE were reached at pH 10, i.e., in runs from 8 to 10 (FE from 74 to 89.8%, Table 3) under conditions of significant Ca^{2+} precipitate formation (T > 2.64, Table 2) with positive ZP (ZP > 9.2 mV, Table 2). Flocculation experiments carried out at pH 12 resulted in similar observations (Tables 2 and 3).

The results are summarized as a response surface created by a quadratic model simulating the flocculation efficiencies (FEs) as a function of the T and ZP of Ca^{2+} precipitate particles (Fig. 1a). As can be seen from Fig. 1a, FE of *M. aeruginosa* cells induced by positively charged Ca^{2+} precipitates almost linearly increased with T. Ca^{2+} precipitates with strongly negative ZP (− 26.8 mV) did not induce flocculation in run 14 (Tables 2 and 3) despite a high T (7.76). Multiple regression analysis of FE data for *M. aeruginosa* flocculation induced by Ca^{2+} precipitates had low *p* values ($p = 0.001$), indicating the significance of the model. The equation expressed in terms of actual factors is:

$$FE = -10.0346 + 28.6232 \times T + 1.5149 \times ZP - 2.5434 \times T^2 + 0.1865 \times T \times ZP + 0.032 \times ZP^2$$

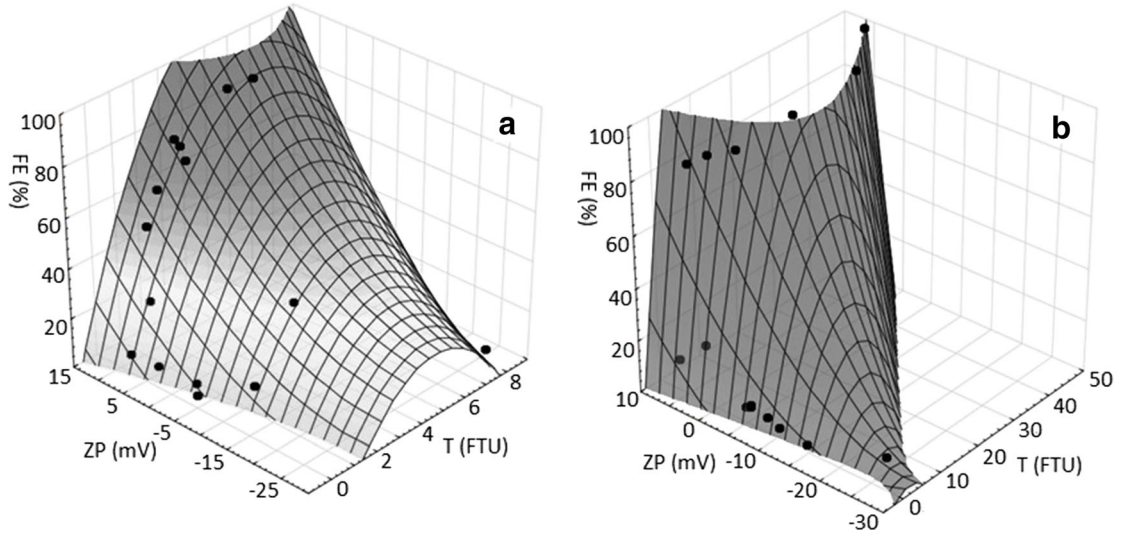

Fig. 1 Flocculation efficiency (FE, Table 3) as a function of turbidity (T, Table 2) and zeta potential (ZP, Table 2) of Ca^{2+} (**a**) and Mg^{2+} precipitate particles (**b**)

Flocculation with Mg^{2+} precipitates differed from that induced by Ca^{2+} precipitates in the following cases. In run 5, a lower FE was achieved with Mg^{2+} compared to Ca^{2+} (4.8% and 64.1%, respectively, Table 3) due to negative ZP and low T of Mg^{2+} precipitates (Table 2). In run 8, the lower FE for flocculation with Mg^{2+} (FE = 20.9%) can be ascribed to lower T as compared to Ca^{2+} precipitate turbidity under the same conditions (0.92 vs 2.64, Table 2). The effect of T was also enhanced by more positive ZP of Ca^{2+} as compared to Mg^{2+} precipitates (10.4 vs 2.6 mV, Table 2). Similar behaviors were observed in the case of runs 11 and 12, where the differences in ZP and T (Table 2) resulted in higher FE induced by Mg^{2+} precipitates (Table 3).

A quadratic model simulating the flocculation efficiencies (FE) as a function of T and ZP of Mg^{2+} precipitate particles was also created (Fig. 1b). It shows that to induce flocculation, a positive ZP of Mg^{2+} precipitate was not a sufficient condition, but it was necessary to also obtain high T (Fig. 1b). Multiple regression analysis of FE data for *M. aeruginosa* flocculation induced by Mg^{2+} precipitates had low p values ($p = 0.01$), indicating the significance of the model. The equation expressed in terms of actual factors is:

$$FE = 22.3586 + 10.7565 \times T + 2.7596 \times ZP - 0.235 \times T^2 + 0.3316 \times T \times ZP + 0.0702 \times ZP^2$$

Modified flocculation tests of *M. aeruginosa* with Ca^{2+} and Mg^{2+} precipitates in the presence of Z8 medium components was tested in runs 10 and 9, respectively. The FE was improved (statistically not significant) in the presence of Z8 medium components by 7.1 and 11.0% for Ca^{2+} and Mg^{2+}, respectively (Table 3).

The impact of cellular organic matter (COM) on flocculation was also quantified. The COM consisted of 63% peptide/protein fraction (37% non-peptides). The effect of COM was tested at pH 10 in runs 9 and 10. FE was significantly ($p < 0.05$) affected by COM (Table 3). The effect of COM on FE was also tested at pH 12 in runs 12 and 15 (Table 3). Here, the presence of COM also led to a decrease in FE. However, the values did not differ significantly ($p > 0.05$) from the corresponding tests without COM.

Prediction of colloidal interactions

The interactions between *M. aeruginosa* cells and Ca^{2+} and Mg^{2+} precipitates were studied with DLVO models using the sphere-sphere approximation. The simulations were carried out under conditions corresponding to the experiments in order to quantify the forces contributing to interaction energies. The Hamaker constant was estimated at 0.8 kT (van Oss 1995), while the mean diameter (4.56 ± 0.12 μm) and circularity (0.87 ± 0.02) of *M. aeruginosa* cells were determined by image analysis. The diameter of precipitates used in DLVO models was 100 nm, which is the precipitate size at the initial nucleation phase.

The G_{DLVO} between *M. aeruginosa* and precipitate particles in run 9 predicted a strong electrostatic attraction (ZP_{cell} = − 31 mV, ZP_{Ca} = 11.1 mV) leading to unhindered contact of cells with precipitate particles (Fig. 2). Under these conditions, both LW and electrostatic (EL) interactions were attractive, implying high FE. However, the experimental FE (74%) was lower than would be expected, probably due to insufficient Ca^{2+} precipitates (T = 3.0).

When the simulation was carried out for the situation when cells were strongly negatively charged (ZP_{cell} = − 34 mV) and precipitates were only slightly negative (ZP_{Mg} = − 1.5 mV),

the DLVO model predicted no potential energy barrier (Fig. 2, run 15). This, in combination with high Mg^{2+} precipitate formation (T = 34.36), resulted in FE = 99.9% (Table 3).

Under conditions of somewhat more negative precipitate surface charge (ZP_{Ca} = − 6.5 mV, Fig. 2, run 7), the DLVO model predicted a potential energy barrier (2.9 kT at 4 nm separation distance), which resulted in decreased FE = 24.7% (Table 3). Even higher electrostatic repulsion (Fig. 2, run 14, ZP_{cell} = − 52 mV, ZP_{Ca} = − 25.3 mV) resulted in a significant predicted energy barrier (55 kT at 0.8 nm separation distance), which was in accordance with low FE = 6.8% (Table 3). Under these conditions, the LW interactions were still attractive but the electrostatic (EL) interactions were strongly repulsive.

Discussion

Alkaline flocculation can be carried out in the presence of Ca^{2+} or Mg^{2+} and PO_4^{3-} ions, which either remain as unconsumed residuals of the culture medium and/or are supplemented in the medium. Since alkaline flocculation can be considered unsustainable (Vandamme et al. 2013) due to declining phosphate reserves, this work was carried out at low concentrations of PO_4^{3-}. Alkaline flocculation is also considered a low-cost harvesting method that exhibits elevated sensitivity to environmental conditions (Gerardo et al. 2015).

The only solid substance predicted to be precipitated from Ca^{2+} and PO_4^{3-} containing model solutions was hydroxyapatite (HA, $Ca_5(PO_4)_3(OH)$) and the mechanism of alkaline flocculation has long been hypothesized (Sukenik and Shelef 1984). However, experimental results supporting the existence of positively charged Ca^{2+} precipitates and their interactions with negatively charged microalgae has been demonstrated only recently. Likewise, the possible flocculation with negatively charged Ca^{2+} precipitates at an early phase of precipitate seed formation has been both predicted and experimentally confirmed (Branyikova et al. 2018).

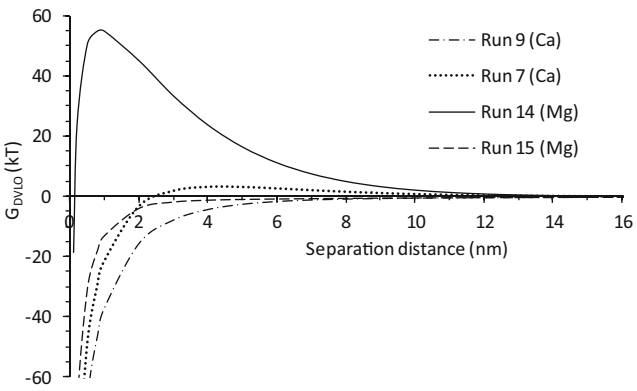

Fig. 2 Total interaction energy (G_{DLVO}) as a function of the separation distance between Ca^{2+} or Mg^{2+} precipitates and *M. aeruginosa* cells during flocculation tests. The description of runs is in accordance with Tables 2 and 3

Somewhat different is the situation with precipitates formed in Mg^{2+} and PO_4^{3-} solutions. According to solubility equilibria, the formation of $Mg_3(PO_4)_2$ starts at pH 8.6 (0.028 mmol L^{-1}, Mg^{2+} and PO_4^{3-} levels at + 1, see Table 1). At pH 9.9, Visual MINTEQ predicts the formation of another precipitate—brucite ($Mg(OH)_2$, equilibrium amount 1.72×10^{-3} mol L^{-1}), which turns into a single solid precipitate species at pH 10.7 (equlibrium amount of brucite 5.39×10^{-3} mol L^{-1}) and above. Consequently, the precipitates formed in model solutions will be referred to as Mg^{2+} precipitates.

Given that alkaline flocculation has been reported to result in cell lysis (Vandamme et al. 2012), it would be advantageous to carry out the process at the lowest alkaline pH possible. However, at pH 8, the FE with Mg^{2+} precipitates was very low (max. 6.6 %), while with Ca^{2+} precipitates, the maximum was 64.1% (run 5, Table 3). Technologically acceptable levels of FE were achieved at pH 10 for Ca^{2+} (89.8%) and Mg^{2+} (92.5%) precipitate-induced flocculation, both in run 10 (Table 3). The difference between these two FEs was statistically not significant ($p > 0.05$). At pH 12, the highest FE for Ca^{2+} precipitates were achieved in run 15 (95.5%, Table 3), when sufficient positively charged precipitates (T = 4.08) were formed (Table 2). For Mg^{2+} precipitates, the massive brucite formation at pH 12 (maximum T = 47.36, Table 2) resulted in high FE (94.5–99.9%), except in run 14, when the Mg^{2+} precipitates were negatively charged (Table 2), due to high PO_4^{3-} and low Mg^{2+} concentrations available for precipitate formation. This is in agreement with the finding that Mg^{2+} was capable of inducing alkaline flocculation in the absence of PO_4^{3-}. The same does not apply for Ca^{2+} (Vandamme et al. 2012). Consequently, the FE achieved with Mg^{2+} was high over a significantly broader range of PO_4^{3-} concentrations than Ca^{2+}. The positive surface charge of $Mg_3(PO_4)_2$ and brucite (at pH below 11) can be expected (Brady et al. 2014) as was confirmed by precipitate ZP at pH 10 in this work (Table 2). However, brucite (MgO^-) can also have a negative surface charge at a pH above 11 (Brady et al. 2014). This was confirmed by all ZP measurements of Mg^{2+} precipitates at pH 12, except for run 12 (ZP_{Mg} = 2.1 mV, Table 2).

The DLVO model of interaction between slightly negative ZPs of Mg^{2+} precipitates (up to − 2.0 mV) with negatively charged *M. aeruginosa* cells did not result in a potential energy barrier preventing adhesion. This was subsequently verified experimentally with high FE at pH 12 (runs 11, 13, and 15, Tables 2 and 3). Based on the data obtained in this work, it can be hypothesized that under our model conditions, alkaline flocculation induced by positively charged $Mg_3(PO_4)_2$ precipitates at pH > 8.6 has a prevailing electrostatic (charge neutralization) character. This is supported by the mechanism of

sweeping flocculation at pH 12, due to massive brucite formation.

Good agreement was found for flocculation experiments and model predictions. The DLVO predictions in this study were made for precipitate particle diameters of 100 nm (Fig. 2). When the DLVO simulation was carried out for smaller particles (10 nm), the height of the predicted barriers diminished. This means that when the cells are in contact with precipitate particles at an early stage of seed formation, the cell vs particle interaction is even more probable. The DLVO simulation with larger particles (1 μm) gave the opposite results, showing a decreasing probability of favorable cell-particle interactions. This has been clearly demonstrated both theoretically and experimentally when studying alkaline flocculation of *Chlorella vulgaris* (Branyikova et al. 2018). As a practical implication, flocculation induced by a shift to alkaline pH should be carried out in situ with cell suspensions, so that the cells can interact with precipitate particles of the smallest possible diameter.

The results show that FE was improved by the presence of culture medium components at their maximum concentrations in fresh Z8 medium. This improvement had a statistically moderate significance (p = 0.05–0.1). For HA-induced flocculation (run 10, Table 3), the presence of medium components increased the formation of HA by 50% as well as led to the formation of calcite (equilibrium amount 1.84×10^{-4} mol L^{-1}). The prediction for Mg^{2+} precipitation (run 9, Table 3) with medium components resulted in formation of equilibrium amounts of $Mg_3(PO_4)_2$ (6.5×10^{-5} mol L^{-1}), brucite (3.09×10^{-3} mol L^{-1}), HA (7.19×10^{-5} mol L^{-1}), and artinite ($Mg_2(CO_3)(OH)_2 \cdot 3H_2O$, 6.5×10^{-5} mol L^{-1}).

During the cultivation of *M. aeruginosa*, the extracellular algal organic matter in the cultivation medium increased to 55 mg L^{-1} DOC at the beginning of the stationary phase (Pivokonsky et al. 2014). Therefore, the tested COM concentration in this work was 50 mg L^{-1} DOC. The composition of COM isolated in this work was very similar to that characterized in Pivokonsky et al. (2014). The COM from *C. vulgaris* consisted of 95% of non-peptide fractions (5% peptides/proteins) and did not affect FE in a statistically significant way (Branyikova et al. 2018). The disruptive effect of *M. aeruginosa* COM, containing 63% of peptide/protein fraction (37% non-peptides), was statistically significant (p < 0.05) for both Ca^{2+} (72.7%, run 10) and Mg^{2+} precipitates (59.4%, run 9) (Table 3). The titration curves of proteins revealed their negative charge at alkaline pH due to (de)protonation of functional groups ($-COO^-$, $-NH_2$). This led to repulsion between *M. aeruginosa* proteins and negatively charged kaolin particles (Safarikova et al. 2013). The same electrostatic type of interaction can be hypothesized to decrease FE of *M. aeruginosa* through protein-Ca^{2+} (or Mg^{2+}) precipitate interactions, based on electrostatic attraction. To compensate for the disruptive effect of *M. aeruginosa* COM, the flocculation tests were carried out under conditions of massive precipitate formation. Higher Mg^{2+} (run 12, T = 47.36) precipitate formation restored FE at 93.1%. Under these conditions, the *M. aeruginosa* COM are either not able to inactivate all precipitate seeds and/or the sweeping flocculation mechanism improves FE. Alkaline flocculation at pH 12 in the presence of COM can be carried out at low PO_4^{3-} and high Mg^{2+} concentrations (run, 12, Table 3). Thus, the pH shift can be carried out with the addition of $Mg(OH)_2$. The price of $Mg(OH)_2$ (US$100–200 t^{-1}) is comparable with that of slaked lime (US$80–180 t^{-1}, https://www.alibaba.com), which was suggested to be used in Vandamme et al. (2012).

Conclusions

Alkaline flocculation is a promising preconcentration method, and understanding of the effects of cell/precipitate surface charge, turbidity, medium composition, and environmental conditions on flocculation efficiency is important for its practical applications. The results presented here defined the concentration ranges of Ca^{2+}, Mg^{2+}, PO_4^{3-}, and the optimum pH that supported efficient flocculation of *M. aeruginosa*. To reduce the risk of cell damage, alkaline flocculation should be carried out at the lowest alkaline pH possible, together with the use of the lowest possible concentrations of Ca^{2+}, Mg^{2+}, and PO_4^{3-}. Efficient flocculation with Mg^{2+} precipitates is more advantageous because it requires less phosphate.

Funding information This research was supported by the Grant Agency of the Czech Republic (project 18-05007S).

Compliance with ethical standards

Conflict of interest The authors declare that they have no conflict of interest.

References

Brady PV, Pohl PI, Hewson JC (2014) A coordination chemistry model of algal autoflocculation. Algal Res 5:226–230

Branyikova I, Filipenska M, Urbanova K, Ruzicka MC, Pivokonsky M, Branyik T (2018) Physicochemical approach to alkaline flocculation of *Chlorella vulgaris* induced by calcium phosphate precipitates. Colloids Surf B 166:54–60

Folkman Y, Wachs AM (1973) Removal of algae from stabilization pond effluents by lime treatment. Water Res 7:419–435

Geada P, Gkelis S, Teixeira J, Vasconcelos V, Vicente A, Fernandes B (2017a) Cyanobacterial toxins as a high added-value product. In: Muñoz R, Gonzalez C (eds) Microalgae-based biofuels and bioproducts. Woodhead Publishing, Cambridge, pp 405–432

Geada P, Pereira RN, Vasconcelos V, Vicente AA, Fernandes BD (2017b) Assessment of synergistic interactions between environmental factors on *Microcystis aeruginosa* growth and microcystin production. Algal Res 27:235–243

Gerardo ML, Van Den Hende S, Vervaeren H, Coward T, Skill SC (2015) Harvesting of microalgae within a biorefinery approach: a review of the developments and case studies from pilot-plants. Algal Res 11: 248–262

González-Fernández C, Ballesteros M (2013) Microalgae autoflocculation: an alternative to high-energy consuming harvesting methods. J Appl Phycol 25:991–999

Hermansson M (1999) The DLVO theory in microbial adhesion. Colloids Surfaces B 14:105–119

Ito T, Okabe K, Mori M (2018) Growth reduction of *Microcystis aeruginosa* by clay ball elution solution. Appl Clay Sci 162:223–239

Khan MI, Lee MG, Seo HJ, Shin JH, Shin TS, Yoon YH, Kim MY, Choi JI, Kim JD (2016) Enhancing the feasibility of *Microcystis aeruginosa* as a feedstock for bioethanol production under the influence of various factors. Biomed Res Int 2016:1–9

Khan MI, Lee MG, Shin JH, Kim JD (2017) Pretreatment optimization of the biomass of *Microcystis aeruginosa* for efficient bioethanol production. AMB Express 7:1–9

Kolska Z, Reznickova A, Svorcik I (2012) Surface characterization of polymer foils. E-polymers 083:1–13

Lawton LA, Edwards C (2008) Conventional laboratory methods for cyanotoxins. In: Hudnell HK (ed) Cyanobacterial Harmful Algal Blooms: State of the Science and Research Needs. Springer, New York, pp 513–537

Leentvar J, Rebhun ME (1982) Effect of magnesium and calcium precipitation on coagulation-flocculation with lime. Water Res 16:655–662

Lin Z, Xu Y, Zhen Z, Fud Y, Liu Y, Li W, Luo C, Ding A, Zhang D (2015) Application and reactivation of magnetic nanoparticles in *Microcystis aeruginosa* harvesting. Bioresour Technol 190:82–88

Lürling M, Noymac NP, Magalhães L, Miranda M, Mucci M, van Oosterhout F, Huszar VLM, Marinho MM (2017) Critical assessment of chitosan as coagulant to remove cyanobacteria. Harmful Algae 66:1–12

Merel S, Walker D, Chicana R, Snyder S, Baures E, Thomas O (2013) State of knowledge and concerns on cyanobacterial blooms and cyanotoxins. Environ Int 59:303–327

Molina Grima E, Belarbi EH, Acién Fernández FG, Robles Medina A, Chisti Y (2003) Recovery of microalgal biomass and metabolites: process options and economics. Biotechnol Adv 20:491–515

Naceradska J, Pivokonsky M, Pivokonska L, Baresova M, Henderson RK, Zamyadi A, Janda V (2017) The impact of pre-oxidation with potassium permanganate on cyanobacterial organic matter removal by coagulation. Water Res 114:42–49

Nguyen TDP, Frappart M, Jaouen P, Pruvost J, Bourseau P (2014) Harvesting *Chlorella vulgaris* by natural increase in pH: effect of medium composition. Environ Technol 35:1378–1378

Niedermeyer THJ, Daily A, Swiatecka-Hagenbruch M, Moscow JA (2014) Selectivity and potency of microcystin congeners against OATP1B1 and OATP1B3 expressing cancer cells. PLoS One 9: e91476

Paerl HW, Hall NS, Calandrino ES (2011) Controlling harmful cyanobacterial blooms in a world experiencing anthropogenic and climatic-induced change. Sci Total Environ 409:1739–1745

Pivokonsky M, Safarikova J, Baresova M, Pivokonska L, Kopecka I (2014) A comparison of the character of algal extracellular versus cellular organic matter produced by cyanobacterium, diatom and green alga. Water Res 51:37–46

Prochazkova G, Podolova N, Safarik I, Zachleder V, Branyik T (2013) Physicochemical approach to freshwater microalgae harvesting with magnetic particles. Colloids Surf B 112:213–218

Safarikova J, Baresova M, Pivokonsky M, Kopecka I (2013) Influence of peptides and proteins produced by cyanobacterium *Microcystis aeruginosa* on the coagulation of turbid waters. Sep Purif Technol 118:49–57

Shi W, Tan W, Wang L, Pan G (2016) Removal of *Microcystis aeruginosa* using cationic starch modified soils. Water Res 97:19–25

Sukenik A, Shelef G (1984) Algal autoflocculation - verification and proposed mechanism. Biotechnol Bioeng 26:142–147

Tappan E, Chamberlin AR (2008) Activation of protein phosphatase 1 by a small molecule designed to bind to the enzyme's regulatory site. Chem Biol 15:167–174

van Oss CJ (1995) Hydrophobicity of biosurfaces — origin, quantitative determination and interaction energies. Colloids Surf B 5:91–110

Vandamme D, Foubert I, Fraeye I, Meesschaert B, Muylaert K (2012) Flocculation of *Chlorella vulgaris* induced by high pH: role of magnesium and calcium and practical implications. Bioresour Technol 105:114–119

Vandamme D, Foubert I, Muylaert K (2013) Flocculation as a low-cost method for harvesting microalgae for bulk biomass production. Trends Biotechnol 31:233–239

Wang L, Liang W, Yu J, Liang Z, Ruan L, Zhang Y (2013) Flocculation of *Microcystis aeruginosa* using modified larch tannin. Environ. Sci Technol 47:771–5777

Yap RKL, Whittaker M, Diao M, Stuetz RM, Jefferson B, Bulmus V, Peirson WL, Nguyen AV, Henderson RK (2014) Hydrophobically-associating cationic polymers as micro-bubble surface modifiers in dissolved air flotation for cyanobacteria cell separation. Water Res 61:253–262